THE JOURNAL OF BIOLOGICAL CHEMISTRY
Vol. 277, No. 26, Issue of June 28, pp. 23447–23452, 2002
Printed in U.S.A.

Insertion and Topology of a Plant Viral Movement Protein in the Endoplasmic Reticulum Membrane*

Received for publication, March 26, 2002, and in revised form, April 17, 2002
Published, JBC Papers in Press, April 25, 2002, DOI 10.1074/jbc.M202935200

Marçal Vilar‡§, Ana Saurí‡¶, Magnus Monné‖, José F. Marcos, Gunnar von Heijne‖, Enrique Pérez-Payá‡, and Ismael Mingarro‡ ‡‡**

*From the ‡Departament de Bioquímica i Biologia Molecular, Universitat de València, E-46 100 Burjassot, Spain, the ‖Department of Biochemistry and Biophysics, Stockholm University, SE-106 91 Stockholm, Sweden, and the **Departamento de Ciencia de los Alimentos, Instituto de Agroquímica y Tecnología de Alimentos, CSIC, E-46 100 Burjassot, Spain*

Virus-encoded movement proteins (MPs) mediate cell-to-cell spread of viral RNA through plant membranous intercellular connections, the plasmodesmata. The molecular pathway by which MPs interact with viral genomes and target plasmodesmata channels is largely unknown. The 9-kDa MP from carnation mottle carmovirus (CarMV) contains two potential transmembrane domains. To explore the possibility that this protein is in fact an intrinsic membrane protein, we have investigated its insertion into the endoplasmic reticulum membrane. By using *in vitro* translation in the presence of dog pancreas microsomes, we demonstrate that CarMV p9 inserts into the endoplasmic reticulum without the aid of any additional viral or plant host components. We further show that the membrane topology of CarMV p9 is N_{cyt}-C_{cyt} (N and C termini of the protein facing the cytoplasm) by *in vitro* translation of a series of truncated and full-length constructs with engineered glycosylation sites. Based on these results, we propose a topological model in which CarMV p9 is anchored in the membrane with its N- and C-terminal tail segments interacting with its soluble, RNA-bound partner CarMV p7, to accomplish the viral cell-to-cell movement function.

RNA is a structurally versatile molecule, and it performs diverse biological roles in the cells. To fulfill these roles, RNA almost invariably functions in association with proteins. This is true also for RNA transport, where proteins stabilize, protect, and target RNA for passage through the nucleocytoplasmic pores or for intercellular trafficking. However, the functional and structural analysis of the diverse families of RNA-binding proteins is still far from completed.

One of these families of proteins whose mechanism of action has not been fully characterized is the movement protein (MP)[1] family found in plant viruses. The process of infection by plant viruses depends on the cell-to-cell traffic of viruses within a plant host. This process is mediated by MPs and is assumed to take place through the plasmodesmata. These are membranous channels that connect higher plant cells into a functional intercellular communication network. Many proteins, including several plant virus MPs (1), have been reported to be associated with these specialized channels and to facilitate passage of a variety of macromolecules into and between cells and cellular compartments. Consequently, viral infection spreads throughout the whole host plant (reviewed in Refs. 2–4). The spread of infection is aided by interactions between pathogen and host components (5). Furthermore, several MPs have been demonstrated to increase plasmodesmatal size exclusion limits to allow the movement of virus-nucleic acid complexes into adjacent cells (6, 7).

Although MPs are required for this dramatic and temporary increase in intercellular permeability, the responsible mechanism is so far unclear. However, because of the intrinsic membranous composition of the plasmodesmata, it can be assumed that many of the associated proteins could be membrane proteins. Thus, the MP of the tobacco mosaic virus (TMV), a member of the so-called 30-kDa superfamily of virus MPs (8, 9), contains an integral membrane protein-like domain and a cytosolically exposed RNA-binding domain (10). There is also experimental evidence that supports a predominant role of membrane protein-like domains in other MPs (11–13).

It has been reported that many plant viruses replicate in association with the ER membrane, and in some cases it has been postulated that membrane-integrated MPs would allow the formation of the membrane-associated replication complexes (14–16). MPs would thus contribute to the intracellular distribution of the virus and to the above-mentioned manipulation of plasmodesmal pores to facilitate cell-to-cell spread of infection. Studies aimed at understanding the molecular basis of multi-domain proteins often are confounded by the sheer complexity of such proteins. Our goal is to uncover the dual functions of MPs (RNA binding and membrane interaction) through functional and structural analysis of MPs found in viruses containing multiple single-domain MPs.

Carmoviruses are among the smallest known plant viruses whose MPs do not belong to the multi-domain 30-kDa superfamily. Their genome is a positive sense single-stranded RNA of ~4 kb encoding at least five proteins (17, 18). The type member of the group, carnation mottle carmovirus (CarMV), has in the central region of the genome two small overlapping open reading frames that code for two small MPs, p7 and p9. It has been demonstrated in the closely related turnip crinkle carmovirus that disruption of the homologous genes blocks the cell-to-cell movement function of the virus (19).

* This work has been supported by Grant BMC2000-1448 from the Spanish Ministerio de Ciencia y Tecnología (to I. M.), Grant BIO4-CT97-2086 from the European Union Biotechnology (to E. P.-P.), and grants from the Swedish Cancer Foundation and the Swedish Research Council (to G. v. H.). The costs of publication of this article were defrayed in part by the payment of page charges. This article must therefore be hereby marked "*advertisement*" in accordance with 18 U.S.C. Section 1734 solely to indicate this fact.

§ Supported by a short term European Molecular Biology Organization fellowship during part of this work.

¶ Recipient of a predoctoral fellowship from the Spanish MCyT.

‡‡ To whom correspondence should be addressed. Tel.: 34-96-386-4385; Fax: 34-96-386-4635; E-mail: Ismael.Mingarro@uv.es.

[1] The abbreviations used are: MP, movement protein; CarMV, carnation mottle carmovirus; ER, endoplasmic reticulum; Lep, leader peptidase; TM, transmembrane; TMV, tobacco mosaic tobamovirus; MOPS, 4-morpholinepropanesulfonic acid.

We have previously characterized CarMV p7 as a soluble protein with RNA binding capacity (20) and have structurally characterized, by means of a retrostructural approach, three different protein domains of p7, including the RNA-binding domain (21). Thus, comparing the MPs of Carmoviruses with those of the 30-kDa superfamily (taking as representative TMV MP), p7 should be considered as the equivalent to the cytosolically exposed RNA-binding domain of TMV MP. Therefore, CarMV p9 is a strong candidate for the membrane-embedded domain found in TMV MP.

In the present study, we show that CarMV p9 is an integral membrane protein. Sequence analysis of p9 and homologues from related plant viruses shows two consensus hydrophobic regions, suggesting the presence of two membrane-spanning domains. Peptides corresponding to the two putative transmembrane segments of CarMV p9 have been analyzed by CD spectroscopy, and the membrane inserting activity of the hydrophobic domains has been evaluated by *in vitro* transcription/translation experiments using ER-derived dog pancreas microsomes. In addition, we have used a glycosylation mapping technique to determine the topology of CarMV p9 in the ER membrane. A model is proposed where the RNA is targeted to the membrane through an interaction between p7 and p9. Such a protein complex would facilitate the cell-to-cell viral transport through the plasmodesmata channels.

MATERIALS AND METHODS

Enzymes and Chemicals—Unless otherwise stated, all of the enzymes as well as plasmid pGEM1, RiboMAX SP6 RNA polymerase system, and rabbit reticulocyte lysate were from Promega (Madison, WI) or Roche Molecular Biochemicals. [^{35}S]Met and ^{14}C-methylated marker proteins were from Amersham BioSciences. The PCR purification and RNeasy RNA clean up kits were from Qiagen (Hilden, Germany). The PCR mutagenesis kit QuikChange was from Stratagene (La Jolla, CA). The oligonucleotides were from the Kebo Laboratory (Stockholm, Sweden), Roche Molecular Biochemicals, and Isogen (Maarssen, The Netherlands).

Peptide Synthesis and Purification—Peptides $p9_{3-24}$ and $p9_{36-57}$ were manually synthesized by solid phase peptide synthesis using Fmoc (*N*-(9-fluorenyl)methoxycarbonyl) chemistry (39), and peptide $p9_{56-84}$ was synthesized as a C-terminal carboxamide on a 0.10 mM scale using an Applied Biosystems model 433A solid phase peptide synthesizer. Analytical reversed-phase high pressure liquid chromatography and laser desorption time-of-flight mass spectrometry were used to determine the purity and identity of the peptides.

Circular Dichroism Spectroscopy—All of the measurements were carried out on a Jasco J-810 CD spectropolarimeter in conjunction with a Neslab RTE 110 water bath and temperature controller as in Ref. 21. The secondary structure content was analyzed with the software provided with the spectropolarimeter, which uses as a reference the CD spectra of model proteins (40).

Construction of Lep/p9 Fusions—p9 was cloned into pQE-9K from viral RNA of infected *Chenopodium quinoa* plants by a reverse transcription-PCR approach (23). Plasmids encoding Lep pGEM-Lep-NST and pGEM-Lep-QST were previously generated (41). Introduction of the hydrophobic fragments from the p9 protein into the Lep sequence was carried out by replacing the H2 segment of Lep by PCR amplification of pQE-9K with forward primers containing appropriate restriction sites.

For the LepTM1 construct, residues 59–81 in H2 (see Fig. 2, *top panel*) were replaced by residues 1–29 of p9; for LepTM2, again H2 was replaced by residues 30–59 of p9; and for LepTM1TM2, H2 was also replaced by residues 1–59 of p9. After PCR amplification, the PCR products were purified, digested, and ligated to the corresponding Lep vectors digested with the same enzymes. All of the constructs were confirmed by DNA sequencing.

Construction of Full-length p9 and p9/P2 and p9TM1/P2 Fusions—Cloning into pGEM1 was done using full-length p9 *Nco*I-*Nde*I fragments from pQE-9K. To obtain full-length constructs, transcription of p9 gene was done after PCR using a reverse primer carrying an stop codon at the end of p9 sequence. Construct p9TM1/P2 was obtained by PCR deletion of TM2 and the C terminus of p9.

In Vitro Mutagenesis—In constructs LepTM1TM2 and full-length p9, the nucleotide sequence coding for Ala^{44}-Leu^{45}-Ser^{46} (numbering corresponding to the p9 wild type sequence) roughly located in the middle of the second TM fragment was changed to the sequence coding for Glu-Glu-Glu, with the aim of obtaining a nontransmembrane segment as a control for membrane insertion (see "Results"). In the full-length p9 constructs, the nucleotide sequence coding for the Asn-Tyr-Ser glycosylation acceptor site at position 65–67 in the wild type protein was changed to the nonacceptor Gln-Tyr-Ser, whereas an Asn-Ser-Ser was introduced at codons 69–71 replacing the wild type Asp-Ser-Ser sequence (p9WT* construct), roughly 14 amino acids downstream of putative second TM fragment. For mutagenesis, the QuikChange kit was used according to the manufacturer's protocol from Stratagene. DNA mutations were confirmed by DNA sequencing.

In Vitro Transcription and Translation in Reticulocyte Lysate—*In vitro* transcription of Lep constructs was done as previously (24, 42). The reactions were incubated at 37 °C for 2 h. The mRNAs were purified using a Qiagen RNeasy clean up kit and verified on a 1% agarose gel.

In vitro translation of the mRNA synthesized from the *in vitro* transcription was done in the presence of reticulocyte lysate and [^{35}S]Met. The Lep constructs were processed as described previously (24, 42). For p9 constructs, after completion of the translation, the samples were alkaline extracted (see below) and electrophoresed by 12% SDS-PAGE, and the assay was repeated in the presence either of a glycosylation acceptor tripeptide Ac-Asn-Tyr-Thr-NH_2 as described (43) or of a nonacceptor tripeptide Ac-Gln-Tyr-Thr-NH_2 (33 μM in both cases). For endoglycosidase H treatment, the translation mix was diluted (1:3) with 70 mM sodium citrate (pH 5.6) and ultracentrifugated (100,000 × *g* for 20 min) onto a sucrose cushion; pellet was redissolved in 40 μl of the same buffer with 0.5% SDS, 1% β-mercaptoethanol and boiled for 5 min; and the aliquots were then incubated at different times with 0.1 milliunits of endoglycosidase H at 37 °C as described (30).

Alkaline Extraction of Microsomes—The alkaline flotation assays were performed as described (44). For the alkaline extraction experiments, 10 μl of the *in vitro* translation mixture was added to 90 μl of 100 mM Na_2CO_3 (pH 12.5) and incubated on ice for 20 min. This mixture was layered onto a 50-μl sucrose cushion and centrifuged at 100,000 × *g* for 10 min (Beckman TL 100 centrifuge). The pellet was resuspended in 40 μl of SDS-PAGE sample buffer and heated to 95 °C for 5 min while shaking prior to analysis by SDS-PAGE. The supernatant was carefully removed, acid-precipitated by the addition of trichloroacetic acid to 10%, and incubated at 4 °C for 10 min. The precipitate was pelleted by centrifugation in a Microfuge, washed with acetone, dried, and similar to above resuspended in SDS-PAGE sample buffer. All of the gels were dried at 80 °C and scanned using a Fuji BAS1000 PhosphorImager using the MacBAS 2.31 software.

RESULTS

Sequence Analysis of CarMV p9—Sequence comparisons of p9 from CarMV and related plant viral homologues (Fig. 1*A*) show two consensus hydrophobic regions linked by a polar loop, suggesting the presence of two membrane-spanning (TM) domains and a third highly charged region at the C terminus of the protein. TM domain predictions generated by different algorithms also identify two segments with high TM propensity. As an example, Fig. 1*B* shows the probability of each residue to be part of a TM fragment using the TMHMM 2.0 program (22), a method that uses a hidden Markov model for predicting TM helices in protein sequences. The first putative TM fragment extends from Asn^{5} to Leu^{23}. Residues Arg^{24}–Ser^{32} define an extramembranous loop, whereas the second TM fragment extends from Leu^{33} to Ile^{55}. The polar C-terminal domain (Ser^{56}–Lys^{84}) is predicted to form a water-soluble region. The loop connecting the two TM domains is rich in polar residues (Ser and Thr) and also contains Pro residues. It is noteworthy that in the more distantly related carmoviruses galinsoga mosaic virus and melon necrotic spot virus (23), only one TM segment is predicted (Fig. 1*A*), which is preceded by polar and Pro residues, suggesting that a putative membrane-anchoring function can be also fulfilled by just one membrane-spanning motif. The same pattern is observed for the four necroviruses sequenced to date (data not shown).

Retrostructural Analyses of CarMV p9—To individually analyze the different p9 regions, we synthesized three different

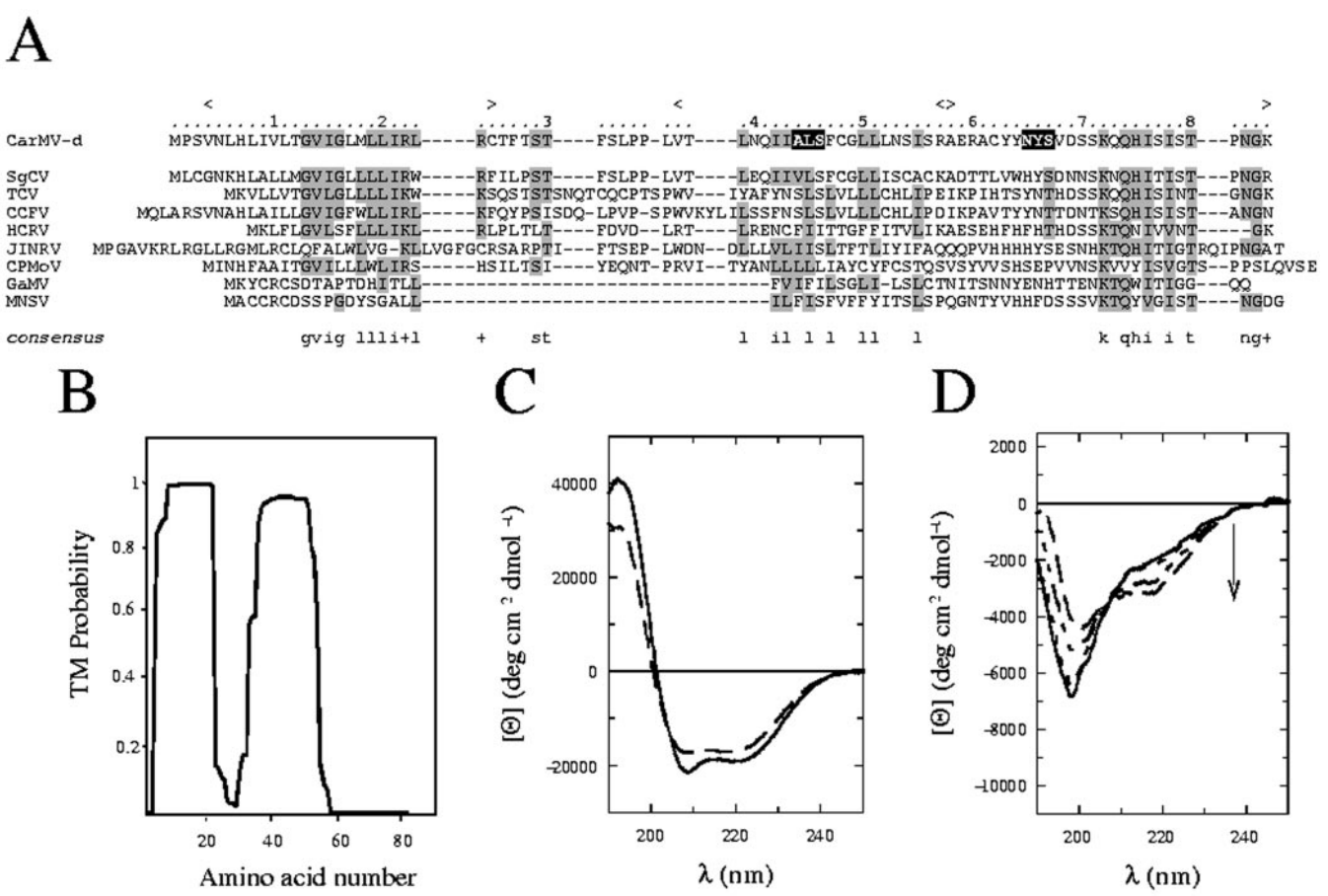

FIG. 1. *A*, sequence alignment of CarMV-dix p9 and related open reading frames from eight carmoviruses. The synthetic peptides (see "Materials and Methods") are shown between *arrowheads* at the *top*. The consensus sequence is shown either as single-letter amino acid codes or as a + symbol, which indicates Lys or Arg. Residues conserved in at least five of the nine sequences are *shaded*. *Black boxes* highlight A44E/L45E/S46E triple mutation and the native glycosylation site at residue 65. *SgCV*, saguaro cactus virus; *TCV*, turnip crinkle virus; *CCFV*, cardamine chlorotic fleck virus; *HCRV*, hibiscus chlorotic ringspot virus; *JINRV*, Japanese iris necrotic ring virus; *CPMoV*, cowpea mottle virus; *GaMV*, galinsoga mosaic virus; *MNSV*, melon necrotic spot virus. *B*, TM probability plot for p9 using TMHMM 2.0 with default parameter settings (22). *C*, far UV CD spectra of the putative TM fragments at 25 μM in 5 mM MOPS/NaOH pH 7.0 buffer solution in the presence of 9 mM SDS. *Solid line*, peptide $p9_{3-24}$; *dotted line*, peptide $p9_{36-57}$. *D*, SDS titration of the C terminus peptide at 50 μM (in the same conditions as in *C*) in 0, 0.1, 0.2, and 0.4 mM SDS. The *descending arrow* indicates increased SDS concentration spectrum.

peptides. Two of them are derived from the putative TM fragment domains (*i.e.* $p9_{3-24}$ and $p9_{36-57}$), and the third one ($p9_{56-84}$) covers the C-terminal domain of the protein. CD analysis of these three peptides in the presence of the secondary structure-inducing solvent trifluoroethanol indicated that peptides $p9_{3-24}$ and $p9_{36-57}$ adopt an α-helical conformation, whereas $p9_{56-84}$ adopts a mixture of random coil and β-sheet conformation (data not shown). In the presence of the membrane-mimetic detergent SDS at micellar concentrations, both $p9_{3-24}$ and $p9_{36-57}$ populate an α-helical conformation (Fig. 1*C*), with a higher helical content for $p9_{3-24}$ (60% α-helix, 11% β-sheet, 3% turn, and 26% random) than for $p9_{36-57}$ (45% α-helix, 19% β-sheet, 2% turn, and 34% random). As expected, the hydrophobic regions identified as putative TM fragments thus behave as hydrophobic α-helices when analyzed in detergent micelles. The β-sheet content in the $p9_{56-84}$ peptide that represents the hydrophilic C-terminal region increases with the SDS concentration from an estimated (see "Materials and Methods") $\approx$60% β-sheet content in aqueous solution to $\approx$72% in the presence of 0.4 mM SDS (Fig. 1*D*).

Insertion of the CarMV p9 α-Helical TM Regions into Biological Membranes—To examine the propensity of the two hydrophobic p9 segments to form TM helices in biological membranes, an *in vitro* translation/translocation system with or without added dog pancreas microsomes was used. The *Escherichia coli* inner membrane protein Lep was used as an insertion vehicle for the putative TM fragments. Lep is anchored in the cytoplasmic membrane by two TM segments (H1 and H2) that are connected by the P1 domain. The P2 domain forms the C-terminal half of the protein (Fig. 2, *top panel*). Upon *in vitro* transcription/translation in the presence of dog pancreas microsomes, Lep has been shown to insert into the microsomal membrane with both the N and C termini on the luminal side (24). An engineered glycosylation site placed downstream of H2 is glycosylated efficiently upon correct insertion into the microsomal membrane, serving as a reporter to distinguish between a lumenal (glycosylated) and a cytoplasmic (unglycosylated) location. Glycosylation of the molecule results in an increase in molecular mass of about 2.5 kDa relative to the observed molecular mass of Lep expressed in the absence of microsomes. The efficiency of glycosylation of Lep under standard conditions is 80–90% (24–26). The microsomal *in vitro* system closely mimics the conditions of *in vivo* membrane protein assembly into the ER membrane.

To study the membrane insertion capacity of the predicted TM fragments, the H2 segment of Lep (Fig. 2, *top panel*) was replaced by the two hydrophobic p9 segments TM1 (residues 1–29, LepTM1) and TM2 (residues 30–59, LepTM2). A segment with membrane insertion capacity will result in glycosylation of the chimeras, whereas a segment that lacks membrane par-

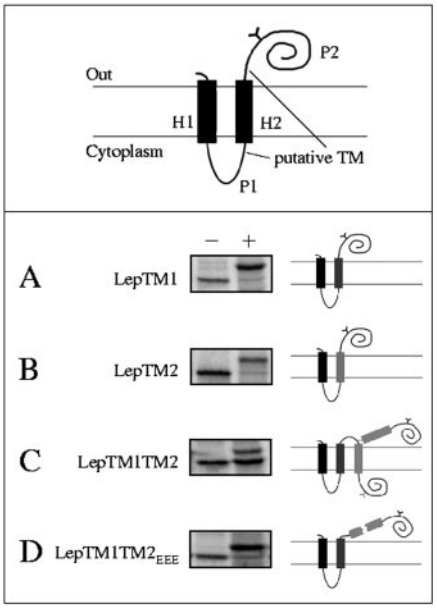

FIG. 2. *Top panel*, membrane topology of Lep. TM segments H1 and H2 are connected by a charged cytoplasmic loop P1. The large periplasmic domain P2 is translocated across the ER membrane. Engineered sites in the coding region of Lep allow the exchange of H2 for p9 fragments and efficient glycosylation. *Bottom panel*, p9 putative TM fragments insert into the microsomal membrane both individually and as a loop-linked sequences. SDS-PAGE analysis of the Lep derived constructs containing: TM1 (*A*), TM2 (*B*), TM1TM2 (*C*), and TM1TM2 carrying the A44E/L45E/S46E mutation (*D*) from p9. All of the constructs were expressed *in vitro* in reticulocyte lysate in the absence (−) and in the presence (+) of rough microsomes. *Black Y-shaped symbol*, glycosylated site; *gray Y-shaped symbol*, unglycosylated site.

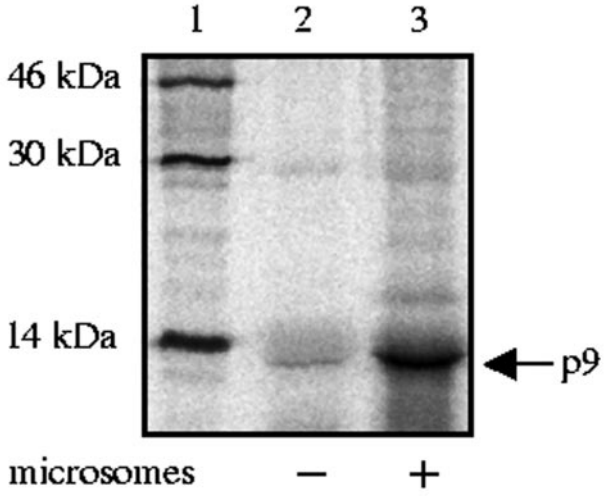

FIG. 3. **SDS-PAGE analysis of alkaline extracted CarMV p9.** *Lane 1*, molecular markers. *Lanes 2* and *3*, p9 translation in the absence and presence, respectively, of microsomal membranes.

titioning will render unglycosylated molecules. Translation of the LepTM1 and LepTM2 constructs in the presence of microsomes resulted in efficient glycosylation, unequivocally demonstrating a transmembrane disposition for both TM1 and TM2 (Fig. 2, *bottom panel*, *A* and *B*). Control constructs with a mutated, nonfunctional glycosylation site (QST in place of NST; see "Materials and Methods") were not glycosylated (data not shown).

When both TM fragments and the native interconnecting loop in CarMV p9 (residues 1–59) replaced the H2 segment of Lep (construct LepTM1TM2), the level of glycosylation dropped to 25% (Fig. 2, *bottom panel*, *C*), suggesting that the predominating topology of this construct is N_{lum}-C_{cyt} with a minor fraction of the molecules having TM2 translocated to the luminal side. A similar level of glycosylation was also observed in a construct where H1 of Lep was not present, *i.e.* when p9 was fused directly to the P2 domain of Lep (construct p9/P2; data not shown). The somewhat inefficient membrane-anchoring ability of the second TM fragment of p9 correlates well with a diminished tendency to populate the α-helical conformation in SDS when compared with the first TM fragment of p9 (Fig. 1*C*).

To verify that the glycosylated LepTM1TM2 molecules result from inefficient membrane anchoring of TM2, we made an additional construct where the hydrophobic residues Ala^{44}-Leu^{45}-Ser^{46} located roughly in the middle of TM2 were changed to Glu^{44}-Glu^{45}-Glu^{46} ($LepTM1TM2_{EEE}$) to totally prevent membrane insertion of this segment. As expected, $LepTM1TM2_{EEE}$ was fully glycosylated (Fig. 2, *bottom panel*, *D*).

CarMV p9 Is an Integral Membrane Protein—Once it was demonstrated that both putative TM fragments from p9 can insert into the ER-derived microsomal membrane using Lep as vehicle, we sought to study the partitioning into the membrane of the wild type p9 protein. Although MPs lack apparent ER signal sequences and previous *in vitro* translated TMV MPs did not associate with dog pancreas membranes (14), transcription/translation products of CarMV p9 showed protein association with heterologous microsomal membranes when analyzed by a flotation assay (Fig. 3). CarMV p9 was quantitatively recovered in the alkali-extracted membrane pellet, whereas only background levels were found in samples assayed in the absence of microsomes, demonstrating proper assembly into the microsomal membrane. Taken together, these results (Figs. 1–3) identify p9 as a bitopic α-helical integral membrane protein.

CarMV p9 Topology in the ER Membrane—The relative orientation of protein membrane-spanning segments is of crucial importance to achieve correct membrane assembly that will allow proper function. The membrane topology predictions derived from p9 are contradictory. We used four well known topology prediction methods. All of them are designed to identify potential TM α-helices and to predict the overall in-out orientation of the protein in the membrane. Although PHD 2.1 (27) and TMHMM 2.0 (22) predict p9 with its N and C termini in the cytoplasm, TOPPRED 2.0 (28) and HMMTOP 2.0 (29) predict the opposite orientation, *i.e.* with the N and C termini in the lumen.

To investigate the actual topology of p9, we first address the targeting and membrane insertion capability of the first TM fragment (TM1) by constructing a fusion where the Lep P2 domain (with a glycosylation site) was fused downstream of TM1 (p9TM1/P2). The results shown in Fig. 4 clearly demonstrate N_{cyt}-C_{lum} orientation for this construct, in agreement with the PHD 2.1 and TMHMM 2.0 predictions.

We next made glycosylation assays of full-length p9 followed by alkaline extraction to study the complete topology of CarMV p9 in the ER membrane. Although there is an endogenous glycosylation site at Asn^{65}-Tyr^{66}-Ser^{67} in p9 (Fig. 1*A*), we decided not to use this sequon as a topological marker, because the distance between TM2 and the target Asn^{65} may be too short to allow efficient glycosylation (24). Asn^{65} was mutated to nonacceptor Gln, and a new glycosylation site was introduced at a more favorable position (Asn^{69}-Ser^{70}-Ser^{71}; construct p9WT*). p9WT* was not glycosylated when translated in the presence of microsomes (Fig. 5*A*, *lane 2*), in agreement with the expected N_{cyt}-C_{cyt} topology. To show that the Asn^{69}-Ser^{70}-Ser^{71} site can be glycosylated if translocated to the ER lumen, we also made a construct where TM2 carried the previously described Ala^{44}-Leu^{45}-Ser^{46}/Glu^{44}-Glu^{45}-Glu^{46} mutation

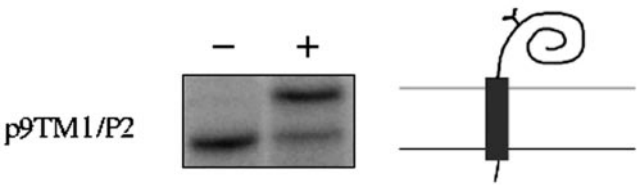

FIG. 4. **TM1 inserts into the microsomes with N_{cyt}-C_{lum} topology.** Residues 1–81 from Lep were replaced by residues 1–29 from p9 (*p9TM1/P2*). As before, *in vitro* expression was performed in reticulocyte lysate either in the absence (−) or the presence (+) of rough microsomes.

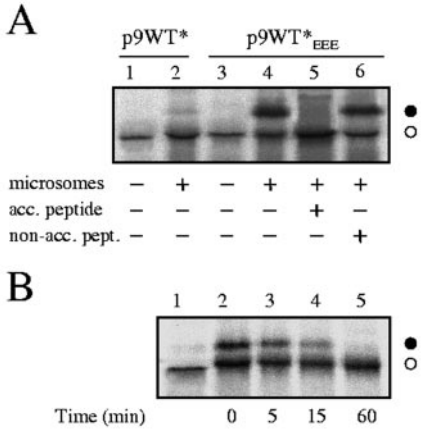

FIG. 5. **Full-length p9 expression *in vitro*.** Expressed p9 sequence (*p9WT**) differs from wild type by a double mutation N65Q/S69N. The p9WT* sequence carrying the A44E/L45E/S46E mutation was named $p9WT^*_{EEE}$. Unglycosylated and glycosylated forms are indicated by *empty* and *filled circles*, respectively. *A*, *lanes 1* and *3*, expressed in the absence of microsomes; *lanes 2* and *4–6*, expressed in the presence of microsomes. In *lanes 5* and *6*, translations were made in the presence of an acceptor peptide and in the presence of a nonacceptor peptide respectively (see "Materials and Methods"). *B*, the $p9WT^*_{EEE}$ construct was translated *in vitro* in the absence (*lane 1*) and in the presence of microsomes (*lanes 2–5*) and digested with 0.1 milliunit of endoglycosidase H with increasing incubation times. *acc.*, acceptor; *pept.*, peptide.

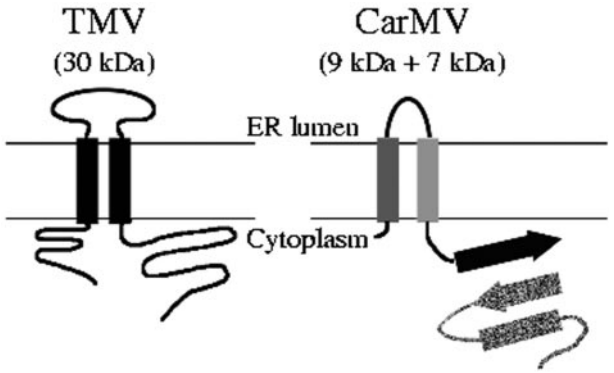

FIG. 6. **Comparative topological model of MPs from TMV and CarMV.** 30-kDa MP from TMV cartoon is depicted from the topological model suggested by Brill *et al.* (10). CarMV MPs are outlined as deduced from data previously reported on p7 characterization (21) and p9 topology in the membrane from this work. α-Helical domains are depicted as *rectangles*, and β-sheets are depicted as *arrowed lines*.

($p9WT^*_{EEE}$) that prevents membrane integration of TM2. Translation of this construct in the presence of microsomes resulted in an increase in the molecular mass (Fig. 5*A*, *lane 4*) that could be blocked by inclusion of a glycosylation inhibitor (Fig. 5*A*, *lane 5*) and by treatment with endoglycosidase H (Fig. 5*B*), a glycan-removing enzyme (30). The glycosylation level obtained for $p9WT^*_{EEE}$ (~60%; Fig. 5, *A*, *lane 4*, and *B*, *lane 2*) is consistent with the somewhat reduced level of glycosylation expected for a target Asn located only 15 residues upstream of the stop codon (31). The efficient glycosylation of p9TM1/P2 and the lack of glycosylation of p9WT* unequivocally demonstrate that the orientation of CarMV p9 is N_{cyt}-C_{cyt}.

DISCUSSION

The mechanism of cell-to-cell transport of plant viruses is unsolved. It has been suggested that MPs may participate in the establishment of membrane-associated replication complexes, affect the intracellular distribution of plant virus, and modify the properties of plasmodesmal pores to allow cell-to-cell spread of infection (4, 32–34). The 30-kDa MP from TMV has been shown to be essential for cell-to-cell spread of the virus (35), and a topological model for this protein with two putative α-helical TM domains and a cytosolically exposed C terminus has been proposed (10). We have previously suggested that the two MPs p7 and p9 from carmoviruses provide a simple model system to study structure/function relationships of plant virus MPs (20), given their small size and separate functions (Refs. 20 and 21 and the present work). RNA binding properties were demonstrated for CarMV p7 (20), and recently we used a retrostructural approach to show that the protein is divided into three structural (and likely functional) domains (21): a variable and unstructured N terminus, a central helical RNA-binding domain, and a very conserved C terminus that folds into a β-sheet. In the present work, we demonstrate that its partner CarMV p9 is an intrinsic membrane protein with two transmembrane helices and N_{cyt}-C_{cyt} topology.

The results obtained for TMV MP and CarMVp9 reveal a membrane-spanning character of MPs with a likely relevant role in the mechanism of plant virus infection. TMV MP behaves as an integral membrane protein because it has been shown that treatment with salts or urea does not release its association with ER isolated from infected cells (34). Our data show that CarMV p9 is similarly difficult to dissociate from ER microsomes into which it was inserted *in vitro*. It has been suggested that TMV MP uses the ER for transport from the sites of viral synthesis to plasmodesmata (14), which in fact do contain ER, and viral infection promotes dramatic morphological changes in ER. However, the targeting of TMV MP to ER is not understood. Like many other plant viral MPs, it does not contain an apparent ER signal sequence (36). Moreover, *in vitro* translation experiments of TMV MP in the presence of membranes, similar to those described in the present study, failed to detect association with membranes (cited in Ref. 14). In fact, it has been hypothesized that the association of TMV MP with a host-encoded and cell wall-associated pectin methylesterase may provide a location signal *in trans* to deliver the MP to its site of action (37). To our knowledge, ours is the first report that demonstrates that a plant viral MP contains in its amino acid sequence all of the molecular information required for its targeting and integration into a biological membrane in the absence of additional viral or plant host proteins/components. Furthermore, the first TM1 segment of p9 is sufficient to drive the targeting and insertion into the ER membrane (as deduced from the membrane insertion experiments using the protein chimera p9TM1/P2; Fig. 4).

There is a need for topological determination and structural characterization of MPs that will help to unravel the virus movement mechanism(s). The actual topology of CarMV p9 in membranes, as deduced from our experimental data using full-length constructs, shows clearly that p9 is anchored in the membrane through two membrane-spanning domains with its N terminus and, chiefly, its C terminus facing the cytoplasm. This particular topological arrangement allows the highly

charged C terminus of p9 to be fully accessible toward the cell cytoplasm.

In the absence of three-dimensional data and given the difficulty of such studies on a membrane protein, we have further characterized CarMV p9 using a retrostructural approach based on three synthetic peptides that cover most of the CarMV p9 sequence. As expected, the two hydrophobic segments both adopt an α-helical conformation in a membrane-mimetic environment, and TM1 (*i.e.* the "targeting" domain) has even higher helical propensity than TM2 (Fig. 1*C*). The C-terminal domain of the protein, which is highly polar (with an abundance of Ser and Thr residues) and has a region well conserved in terms of amino acid sequence (Fig. 1*A*), showed a CD spectrum indicative of low secondary structure content that can be induced to fold into a β-sheet in a membrane mimetic environment (Fig. 1*D*).

We have previously reported that CarMV p7 also has a highly conserved β-sheet C-terminal domain (21). Thus, these two conserved β-sheet domains could mediate protein-protein interactions between membrane-bound p9 and its soluble partner p7, either unbound or bound RNA (see our hypothetical model in Fig. 6). It should also be noticed that in the homologous system from turnip crinkle virus, cellular fractionation experiments have shown that turnip crinkle carmovirus p8 (the p7 homologue) is associated with membrane structures both in transgenic and in virus-infected plants (38), although p8 itself does not contain either ER targeting signals or TM domains. In the case of CarMV p7, it has been recently shown that the amount of protein in membrane-associated fractions increases with time after plant infection.[2] In this alluring model, p7 would bind viral RNA, which would induce a conformational change in this soluble protein, unveiling its C terminus, which could then interact with the cytoplasm-exposed C-terminal domain of p9. This RNA-mediated protein-protein interaction would confine the ternary complex to the membrane.

An inference of our model is that although multiple p7 molecules would wrap (and protect) a single viral RNA (as demonstrated *in vitro*) (21), only one monomer of p9 is theoretically required to target the complex to the membrane, and thus lower amounts of this protein would be required. This points to a difference with the TMV system in which the two functions (RNA binding and membrane location) are performed by the same protein and correlates with experimental data on the relative amounts of p7/p9 in the cell. Although p7 and turnip crinkle carmovirus p8 have been detected unambiguously in infected tissue (21, 38), CarMV p9 (or any of its homologues) has not, confirming the lower accumulation predicted by the model. The accumulation differences also relate to the expression strategy of the two genes from a single viral subgenomic RNA in which the p9 open reading frame is located downstream of p7 and far from the 5′ end (17, 18).

In conclusion, the carmovirus two-MP system reproduces the topological model previously suggested for the 30-kDa MP of TMV (10) in which, as is the case for p9, the N and C termini are exposed to the cytoplasm (Fig. 6). In this sense, it is important to emphasize that carmovirus MPs are not included in the 30-kDa superfamily of viral MPs (8, 9), demonstrating similarity of molecular domain organization and protein function in the absence of detectable sequence similarity (23).

[2] V. Pallás, personal communication.

Acknowledgments—We thank IngMarie Nilsson for helpful advice and Cristina Ferrándiz for critical reading of the manuscript.

REFERENCES

1. Pickard, B. G., and Beachy, R. N. (1999) *Cell* **98,** 5–8
2. Carrington, J. C., Kasschau, K. D., Mahajan, S. K., and Schaad, M. C. (1996) *Plant Cell* **8,** 1669–1681
3. Ghoshroy, S., Lartey, R., Sheng, J., and Citovsky, V. (1997) *Annu. Rev. Plant Physiol. Plant Mol. Biol.* **48,** 27–50
4. Aaziz, R., Dinant, S., and Epel, B. (2001) *Trends Plant Sci.* **6,** 326–330
5. Reichel, C., Mas, P., and Beachy, R. N. (1999) *Trends Plant Sci.* **4,** 458–462
6. Oparka, K. J., Prior, D. A., Santa Cruz, S., Padgett, H. S., and Beachy, R. N. (1997) *Plant J.* **12,** 781–789
7. Oparka, K. J., Roberts, A. G., Boevink, P., Santa Cruz, S., Roberts, I., Pradel, K. S., Imlau, A., Kotlizky, G., Sauer, N., and Epel, B. (1999) *Cell* **97,** 743–754
8. Koonin, E. V., Mushegian, A. R., Ryabov, E. V., and Dolja, V. V. (1991) *J. Gen. Virol.* **72,** 2895–2903
9. Melcher, U. (2000) *J. Gen. Virol.* **81,** 257–266
10. Brill, L. M., Nunn, R. S., Kahn, T. W., Yeager, M., and Beachy, R. N. (2000) *Proc. Natl. Acad. Sci. U. S. A.* **97,** 7112–7117
11. Grieco, F., Castellano, M. A., Di Sansebastiano, G. P., Maggipinto, G., Neuhaus, J. M., and Martelli, G. P. (1999) *J. Gen. Virol.* **80,** 1103–1109
12. Solovyev, A. G., Stroganova, T. A., Zamyatnin, A. A., Jr., Fedorkin, O. N., Schiemann, J., and Morozov, S. Y. (2000) *Virology* **269,** 113–127
13. Ward, B. M., Medville, R., Lazarowitz, S. G., and Turgeon, R. (1997) *J. Virol.* **71,** 3726–3733
14. Heinlein, M., Padgett, H. S., Gens, J. S., Pickard, B. G., Casper, S. J., Epel, B. L., and Beachy, R. N. (1998) *Plant Cell* **10,** 1107–1120
15. Mas, P., and Beachy, R. N. (1999) *J. Cell Biol.* **147,** 945–958
16. McLean, B. G., Zupan, J., and Zambryski, P. C. (1995) *Plant Cell* **7,** 2101–2114
17. Qu, F., and Morris, T. J. (1999) in *Encyclopedia of Virology* (Granoff, A., and Webster, R. G., eds) pp. 243–247, Academic Press, Inc., San Diego, CA
18. Russo, M., Burgyan, J., and Martelli, G. P. (1994) *Adv. Virus Res.* **44,** 381–428
19. Hacker, D. L., Petty, I. T., Wei, N., and Morris, T. J. (1992) *Virology* **186,** 1–8
20. Marcos, J. F., Vilar, M., Perez-Paya, E., and Pallas, V. (1999) *Virology* **255,** 354–365
21. Vilar, M., Esteve, V., Pallas, V., Marcos, J. F., and Perez-Paya, E. (2001) *J. Biol. Chem.* **276,** 18122–18129
22. Krogh, A., Larsson, B., von Heijne, G., and Sonnhammer, E. L. (2001) *J. Mol. Biol.* **305,** 567–580
23. Cañizares, M. C., Marcos, J. F., and Pallás, V. (2001) *Arch. Virol.* **146,** 2039–2051
24. Nilsson, I., and von Heijne, G. (1993) *J. Biol. Chem.* **268,** 5798–5801
25. Johansson, M., Nilsson, I., and von Heijne, G. (1993) *Mol. Gen. Genet.* **239,** 251–256
26. Gafvelin, G., Sakaguchi, M., Andersson, H., and von Heijne, G. (1997) *J. Biol. Chem.* **272,** 6119–6127
27. Rost, B., Fariselli, P., and Casadio, R. (1996) *Protein Sci.* **5,** 1704–1718
28. Claros, M. G., and von Heijne, G. (1994) *Comput. Appl. Biosci.* **10,** 685–686
29. Tusnady, G. E., and Simon, I. (1998) *J. Mol. Biol.* **283,** 489–506
30. Braun, P., and von Heijne, G. (1999) *Biochemistry* **38,** 9778–9782
31. Nilsson, I., Witt, S., Kiefer, H., Mingarro, I., and von Heijne, G. (2000) *J. Biol. Chem.* **275,** 6207–6213
32. Tzfira, T., Rhee, Y., Chen, M.-H., Kunik, T., and Citovsky, V. (2000) *Annu. Rev. Microbiol.* **54,** 187–219
33. Lazarowitz, S. G., and Beachy, R. N. (1999) *Plant Cell* **11,** 535–548
34. Reichel, C., and Beachy, R. N. (1998) *Proc. Natl. Acad. Sci. U. S. A.* **95,** 11169–11174
35. Deom, C. M., Oliver, M. J., and Beachy, R. N. (1987) *Science* **237,** 389–394
36. Deom, C. M., Wolf, S., Holt, C. A., Lucas, W. J., and Beachy, R. N. (1991) *Virology* **180,** 251–256
37. Chen, M. H., Sheng, J., Hind, G., Handa, A. K., and Citovsky, V. (2000) *EMBO J.* **19,** 913–920
38. Li, W. Z., Qu, F., and Morris, T. J. (1998) *Virology* **244,** 405–416
39. Fields, G. B., and Noble, R. L. (1990) *Int. J. Pept. Prot. Res.* **35,** 161–214
40. Yang, J. T., Wu, C. S., and Martinez, H. M. (1986) *Methods Enzymol.* **130,** 208–269
41. Nilsson, I., Whitley, P., and von Heijne, G. (1994) *J. Cell Biol.* **126,** 1127–1132
42. van Geest, M., Nilsson, I., von Heijne, G., and Lolkema, J. S. (1999) *J. Biol. Chem.* **274,** 2816–2823
43. Popov, M., Tam, L. Y., Li, J., and Reithmeier, R. A. F. (1997) *J. Biol. Chem.* **272,** 18325–18332
44. Whitley, P., Grahn, E., Kutay, U., Rapoport, T., and von Heijne, G. (1996) *J. Biol. Chem.* **271,** 7583–7586